Electronic Supplementary Information (ESI) for:

A systematic investigation of structural transformation in copper pyrazolato system: A case study

Jing-Huo Chen,[a,b] Donghui Wei,[a] Guang Yang,*[a] Jian-Gong Ma*[b] and Peng Cheng[b,c]

[a] Green Catalysis Center, and College of Chemistry, Zhengzhou University, Zhengzhou, Henan, 450001, P. R. China.

[b] Department of Chemistry and Key Laboratory of Advanced Energy Material Chemistry, College of Chemistry, Nankai University, Tianjin 300071, P. R. China.

[c] State Key Laboratory of Elemento-Organic Chemistry and Collaborative Innovation Center of Chemical Science and Engineering (Tianjin), Nankai University, Tianjin 300071, P. R. China.

E-mail: yang@zzu.edu.cn; mvbasten@nankai.edu.cn

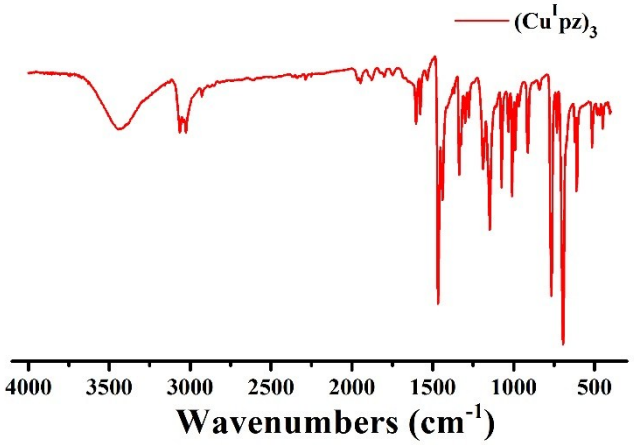

Fig. S1 IR spectrum of complex $(Cu^{I}pz)_3$ in KBr pellet.

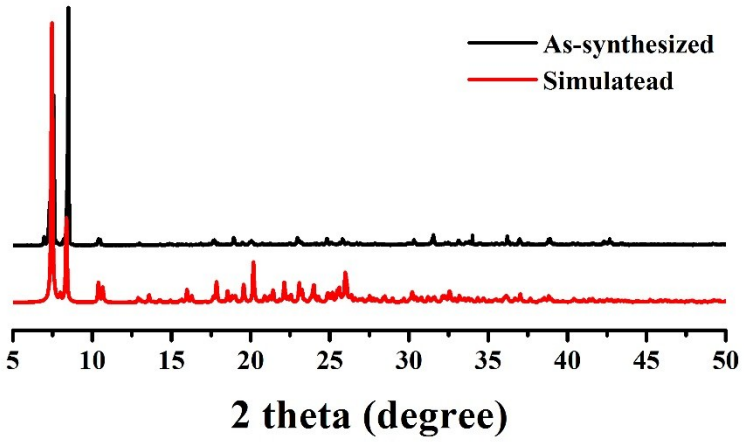

Fig. S2 The P-XRD pattern of $(Cu^{I}pz)_3$ obtained from the as-synthesized sample (black line) and the simulation based on the crystal data (red line).

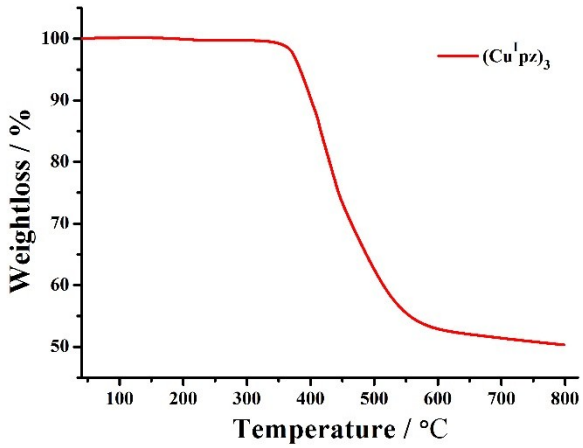

Fig. S3 Thermogravimetric analysis curve of $(Cu^{I}pz)_3$.

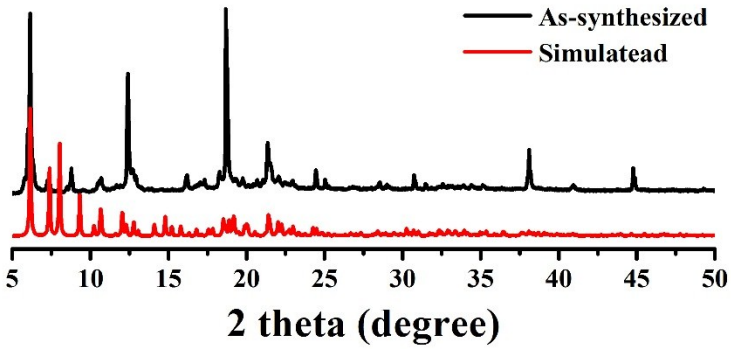

Fig. S4 The P-XRD pattern of **[Cu^{II}pz(OMe)]$_6$** obtained from the as-synthesized sample (black line) and the simulation based on the crystal data (red line).

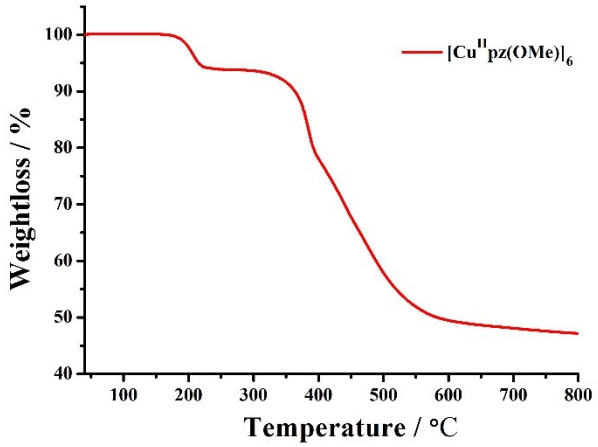

Fig. S5 Thermogravimetric analysis curve of **[Cu^{II}pz(OMe)]$_6$**.

Table S1 Crystallographic data and structure refinements

	$(Cu^{I}pz)_3$	$(Cu^{I}pz)_4$	$Cu^{I}_3Cu^{II}_2(OMe)_2pz_5$	$[Cu^{II}pz(OMe)]_6$
Formula	$C_{45}H_{30}Cl_3Cu_3N_6$	$C_{63.75}H_{47.5}Cl_{11.5}Cu_4N_8$	$C_{77}H_{56}Cl_5Cu_5N_{10}O2$	$C_{96}H_{78}Cl_6Cu_6N_{12}O_6$
Mol. wt.	951.72	1587.43	1648.26	2089.64
Crystal system	Monoclinic	Triclinic	Triclinic	Monoclinic
Space group	$P2_1/c$	P-1	P-1	$P2_1/c$
a (Å)	13.1550(2)	10.0449(2)	16.2557(11)	29.1746(6)
b (Å)	21.1155(3)	15.1382(5)	17.0114(12)	16.6071(4)
c (Å)	14.4734(3)	23.2997(8)	17.9429(11)	19.2602(4)
α (deg)		77.698(3)	72.065(6)	
β (deg)	98.2710(18)	83.790(2)	68.528(6)	100.1273(19)
γ (deg)		80.707(3)	86.629(6)	
V (Å^3)	3978.53(12)	3406.22(19)	4384.9(6)	9186.3(3)
Z	4	2	2	4
T (K)	120(10)	120(10)	120(10)	120(10)
$\rho_{calcd.}$ (Mg/m^3)	1.589	1.548	1.248	1.511
μ (mm^{-1})	1.833	1.728	1.390	1.599
Reflns collected	16007	22985	32709	33733
Reflns unique	7002 (R_{int} = 0.0292)	11906 (R_{int} = 0.0242)	15431 (R_{int} = 0.0797)	16027 (R_{int} = 0.0332)
Final R indices [I> 2σ(I)]	R_1 = 0.0305 wR_2 = 0.0606	R_1 =0.0701 wR_2 = 0.1731	R_1 = 0.0914 wR_2 = 0.2115	R_1 = 0.0407 wR_2 = 0.0889
S	1.023	1.083	1.020	1.023
$\Delta\rho_{max}$(eÅ^{-3})	0.32	1.65	1.55	1.40
$\Delta\rho_{min}$(eÅ^{-3})	-0.28	-1.87	-0.96	-0.65

Table S2 Crystallographic data and structure refinements

	$[Cu^{II}pz(OMe)]_6$-12h	**$[Cu^{II}pz(OMe)]_6$-24h**	**$[Cu^{II}pz(OMe)]_6$-36h**	**$[Cu^{II}pz(OMe)]_6$-48h**	**$[Cu^{II}pz(OMe)]_6$-72h**	**$[Cu^{II}pz(OMe)]_6$-96h**
Formula	$C_{96}H_{78}Cl_6Cu_6N_{12}O_6$	$C_{95}H_{76}Cl_6Cu_6N_{12}O_6$	$C_{189}H_{150}Cl_{12}Cu_{12}N_{24}O_{12}$	$C_{94}H_{74}Cl_6Cu_6N_{12}O_6$	$C_{187}H_{146}Cl_{12}Cu_{12}N_{24}O_{12}$	$C_{92}H_{70}Cl_6Cu_6N_{12}O_6$
Mol. wt.	2089.64	2075.61	4137.20	2061.59	4109.15	2033.54
Crystal system	Monoclinic	Monoclinic	Monoclinic	Monoclinic	Monoclinic	Monoclinic
Space group	*C*2/c	*C*2/c	*C*2/c	*C*2/c	*C*2/c	*C*2/c
a (Å)	29.0762(6)	29.0987(5)	29.0602(6)	29.0564(7)	29.0473(9)	29.0392(8)
b (Å)	16.6019(4)	16.5408(4)	16.4786(6)	16.4701(4)	16.4211(7)	16.3390(8)
c (Å)	19.2306(5)	19.3641(4)	19.3166(4)	19.3195(4)	19.2985(7）	19.2980(6)
α (deg)						
β (deg)	100.045(2)	100.124(2)	100.198(2)	100.272(2)	100.186(3)	100.387(3)
γ (deg)						
V (Å^3)	9140.7(4)	9175.1(3)	9104.0(5)	9097.4(4)	9060.1(6)	9006.3(6)
Z	4	4	2	4	2	4
T (K)	120(10)	120(10)	120(10)	120(10)	120(10)	120(10)
$\rho_{calcd.}$ (Mg/m^3)	1.518	1.503	1.509	1.505	1.506	1.500
μ (mm^{-1})	1.607	1.601	1.613	1.614	1.620	1.629
Reflns collected	17792	16986	17818	18958	17004	16616
Reflns unique	8057 (R_{int} = 0.0198)	8068 (R_{int} = 0.0186)	8001 (R_{int} = 0.0189)	7987 (R_{int} = 0.0223)	7954 (R_{int} = 0.0256)	7907 (R_{int} = 0.0239)
Final *R* indices [$I > 2\sigma(I)$]	R_1 = 0.0421 wR_2 = 0.1038	R_1 = 0.0566 wR_2 = 0.1440	R_1 = 0.0543 wR_2 = 0.1253	R_1 = 0.0451 wR_2 = 0.1012	R_1 =0.0545 wR_2 = 0.1232	R_1 =0.0763 wR_2 = 0.1642
S	1.030	1.038	1.037	1.040	1.063	1.140
$\Delta\rho_{max}$(eÅ^{-3})	0.99	1.68	1.56	1.06	1.04	1.65
$\Delta\rho_{min}$(eÅ^{-3})	-0.98	-1.71	-0.98	-0.66	-0.84	-1.17

Table S3 Selected bond distances (Å) and bond angles (º).

$(Cu^{I}pz)_3$			
Cu(1)-N(1)	1.866(2)	Cu(1)-N(6)	1.865(2)
Cu(2)-N(2)	1.852(2)	Cu(2)-N(3)	1.849(2)
Cu(3)-N(4)	1.867(2)	Cu(3)-N(5)	1.866(2)
Cu(1)···Cu(2)	3.2296(4)	Cu(2)···Cu(3)	3.1403(5)
Cu(1)···Cu(3)	3.2508(5)	N(1)-Cu(1)-N(6)	173.22(9)
N(2)-Cu(2)-N(3)	178.42(9)	N(4)-Cu(3)-N(5)	173.68(9)
$(Cu^{I}pz)_4$			
Cu(1)-N(2)	1.857(5)	Cu(1)-N(3)	1.852(5)
Cu(2)-N(4)	1.846(5)	Cu(2)-N(5)	1.850(5)
Cu(3)-N(6)	1.846(5)	Cu(3)-N(7)	1.845(5)
Cu(4)-N(8)	1.846(5)	Cu(4)-N(1)	1.853(5)
Cu(1)···Cu(2)	3.2228(9)	Cu(2)···Cu(3)	3.0385(11)
Cu(3)···Cu(4)	3.2266(9)	Cu(1)···Cu(4)	3.0933(11)
N(2)-Cu(1)-N(3)	178.6(2)	N(4)-Cu(2)-N(5)	179.2(2)
N(6)-Cu(3)-N(7)	179.1(2)	N(1)-Cu(4)-N(8)	178.4(2)
$Cu^{I}_3Cu^{II}_2(OMe)_2pz_5$			
Cu^{I}(1)-N(1)	1.876(5)	Cu^{I}(1)-N(5)	1.877(5)
Cu^{I}(2)-N(2)	1.888(4)	Cu^{I}(2)-N(3)	1.878(5)
Cu^{II}(3)-N(4)	1.947(5)	Cu^{II}(3)-N(7)	1.962(5)
Cu^{II}(3)-O(1)	1.954(4)	Cu^{II}(3)-O(2)	1.907(4)
Cu^{II}(4)-N(6)	1.937(5)	Cu^{II}(4)-N(10)	1.938(5)
Cu^{II}(4)-O(1)	1.930(4)	Cu^{II}(4)-O(2)	1.925(4)
Cu^{I}(5)-N(8)	1.890(5)	Cu^{I}(5)-N(9)	1.885(5)
Cu^{I}(1)···Cu^{I}(2)	3.5332(12)	Cu^{I}(1)···Cu^{II}(4)	3.0484(12)
Cu^{I}(2)···Cu^{II}(3)	3.0732(12)	Cu^{II}(3)···Cu^{II}(4)	2.9687(12)
Cu^{II}(3)···Cu^{I}(5)	3.1981(11)	Cu^{II}(4)···Cu^{I}(5)	3.1721(13)
N(1)-Cu^{I}(1)-N(5)	175.3(2)	N(2)-Cu^{II}(2)-N(3)	173.3(2)
N(4)-Cu^{II}(3)-O(1)	94.9(2)	N(4)-Cu^{II}(3)-O(2)	164.1(2)
N(7)-Cu^{II}(3)-O(1)	156.2(2)	N(7)-Cu^{II}(3)-O(2)	89.4(2)
N(4)-Cu^{II}(3)-N(7)	102.7(2)	N(6)-Cu^{II}(4)-O(1)	95.7(2)
N(6)-Cu^{II}(4)-O(2)	167.2(2)	N(10)-Cu^{II}(4)-O(1)	157.1(2)
N(10)-Cu^{II}(4)-O(2)	90.1(2)	N(10)-Cu^{II}(4)-N(6)	100.1(2)
N(8)-Cu^{I}(5)-N(9)	173.0(2)		
$[Cu^{II}pz(OMe)]_6$			
Cu(1)-N(1)	1.961(2)	Cu(1)-N(3)	1.965(2)
Cu(1)-O(5)	1.930 (2)	Cu(1)-O(6)	1.919(2)
Cu(2)-N(2)	1.980(2)	Cu(2)-N(4)	1.961(2)
Cu(2)-O(1)	1.911 (2)	Cu(2)-O(2)	1.933(2)
Cu(3)-N(5)	1.960(3)	Cu(3)-N(7)	1.992(2)
Cu(3)-O(1)	1.930(2)	Cu(3)-O(2)	1.911(2)
Cu(4)-N(6)	1.955(2)	Cu(4)-N(8)	1.983(2)

Cu(4)-O(3)	1.924(2)	Cu(4)-O(4)	1.908(2)
Cu(5)-N(9)	1.990(2)	Cu(5)-N(11)	1.963(2)
Cu(5)-O(3)	1.908(2)	Cu(5)-O(4)	1.926(2)
Cu(6)-N(10)	1.973(2)	Cu(6)-N(12)	1.959(2)
Cu(6)-O(5)	1.913(2)	Cu(6)-O(6)	1.924(2)
Cu(1)···Cu(2)	3.1015(8)	Cu(2)···Cu(3)	3.0203(6)
Cu(3)···Cu(4)	2.9847(6)	Cu(4)···Cu(5)	2.9980(8)
Cu(5)···Cu(6)	3.0202(6)	Cu(1)···Cu(6)	3.0208(6)
N(1)-Cu(1)-N(3)	88.69(10)	O(5)-Cu(1)-O(6)	76.15(8)
N(2)-Cu(2)-N(4)	89.06(10)	O(1)-Cu(2)-O(2)	76.31(8)
N(5)-Cu(3)-N(7)	89.28(10)	O(1)-Cu(3)-O(2)	76.38(8)
N(6)-Cu(4)-N(8)	88.13(10)	O(3)-Cu(4)-O(4)	76.94(8)
N(9)-Cu(5)-N(11)	89.33(10)	O(3)-Cu(5)-O(4)	76.87(8)
N(10)-Cu(6)-N(12)	88.24(10)	O(5)-Cu(6)-O(6)	76.43(8)

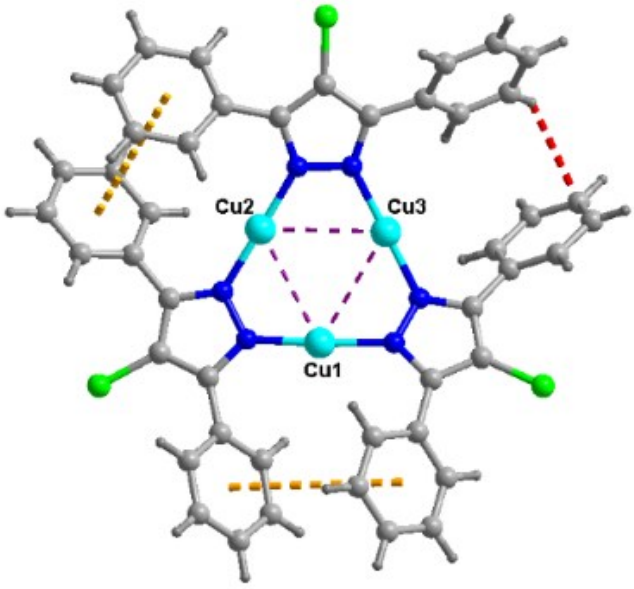

Fig. S6 Ball-and-stick diagram of **$(Cu^{I}pz)_3$** showing the intra-trimer $\pi\cdots\pi$ stacking (dashed yellow lines) and C-H$\cdots\pi$ interactions (dashed red lines) and the Cu$\cdots$Cu interactions (dashed purple lines).

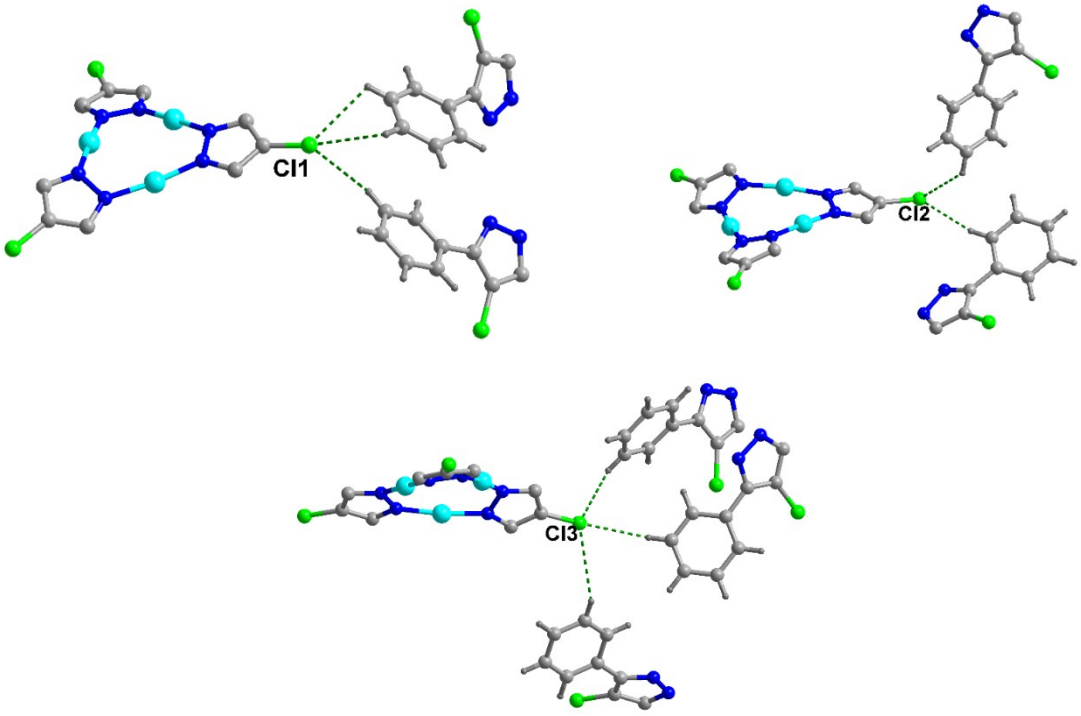

Fig. S7 The intermolecular Cl$\cdots$H(Ph) interactions in **$(Cu^{I}pz)_3$**, some phenyl groups have been omitted for clarity.

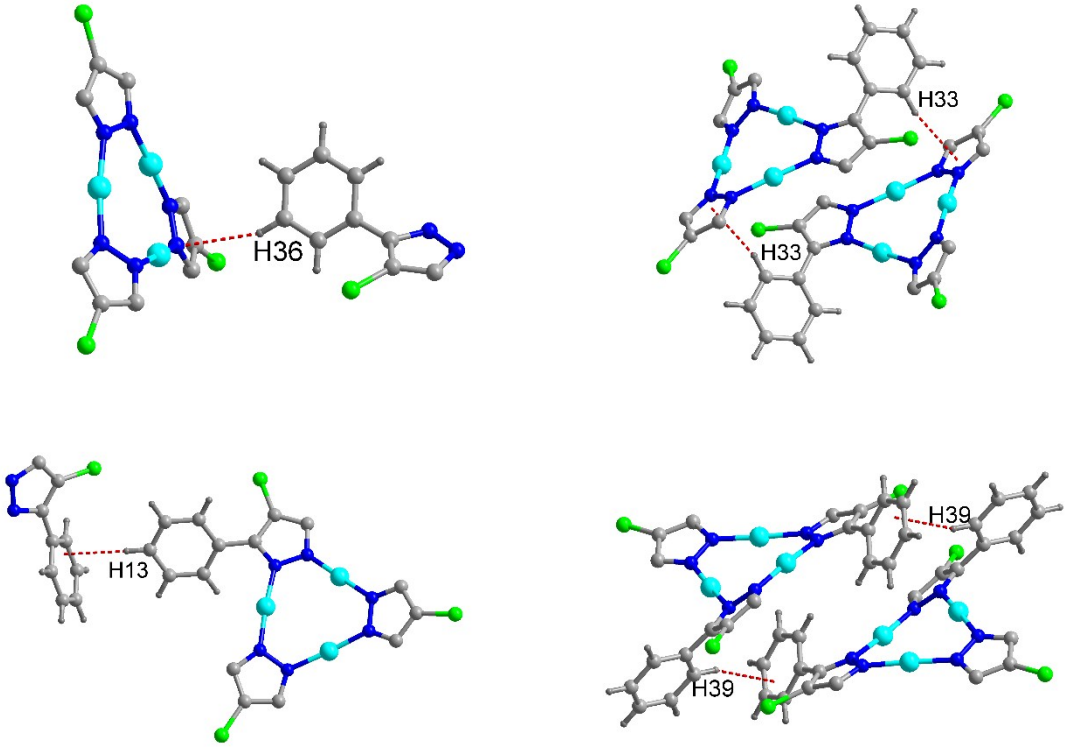

Fig. S8 The intermolecular C-H···π(pz) interaction and C-H···π(Ph) interaction in **$(Cu^{I}pz)_3$**, some phenyl groups have been omitted for clarity.

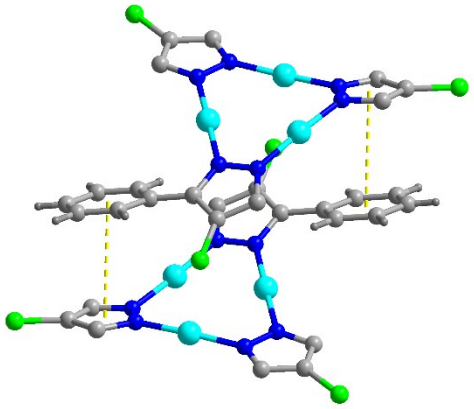

Fig. S9 The intermolecular π(Ph)···π(pz) interaction in **$(Cu^{I}pz)_3$**, some phenyl groups have been omitted for clarity.

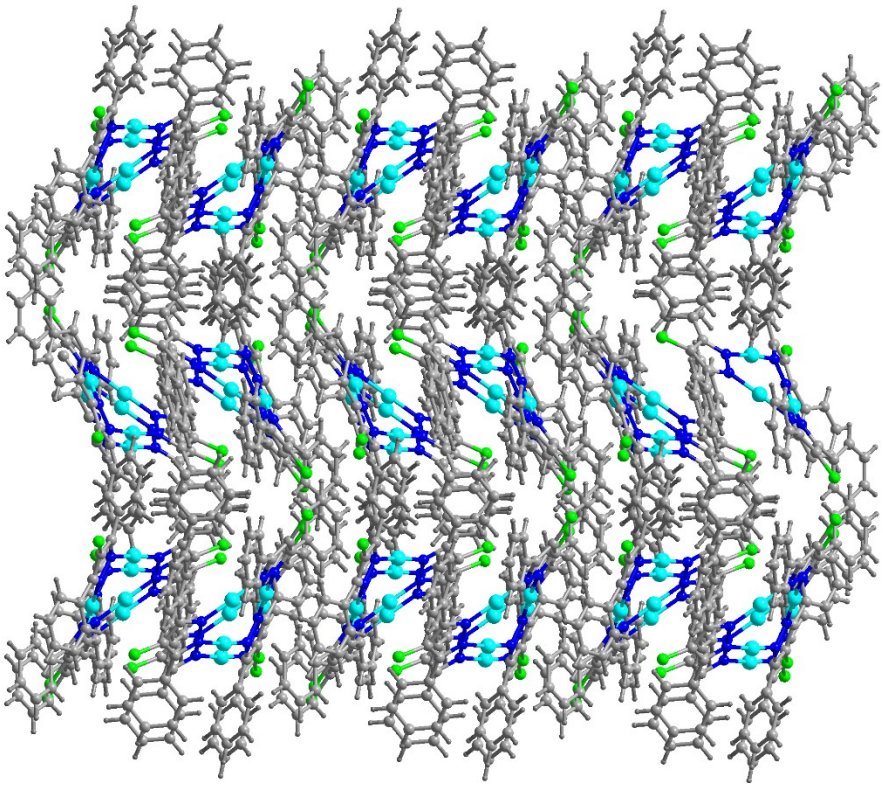

Fig. S10 3-D structure of **$(Cu^{I}pz)_3$** formed *via* the intermolecular C-H···π interactions and Cl···H interactions.

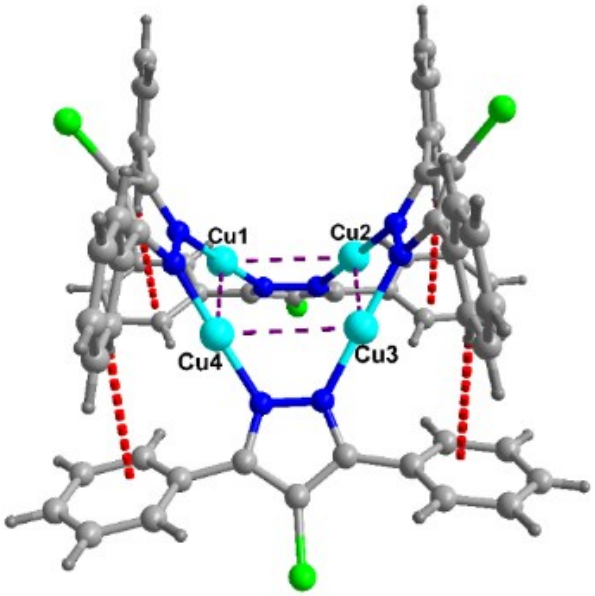

Fig. S11 Ball-and-stick diagram of **$(Cu^{I}pz)_4$**, showing the C-H···π interactions (dashed red lines) and the Cu···Cu interactions (dashed purple lines), the solvent molecules have been omitted for clarity.

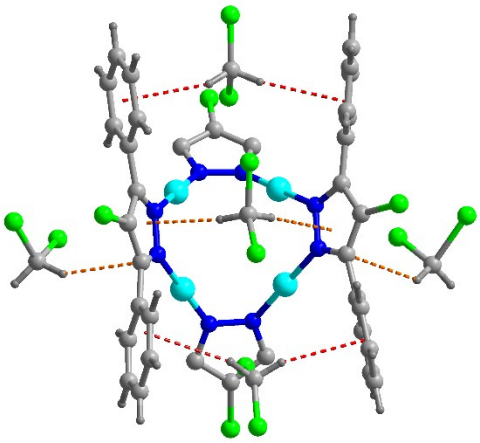

Fig. S12 The intramolecular C(CH_2Cl_2)-H···π(Ph) interaction and C(CH_2Cl_2)-H···π(pz) interaction in **$(Cu^Ipz)_4$**.

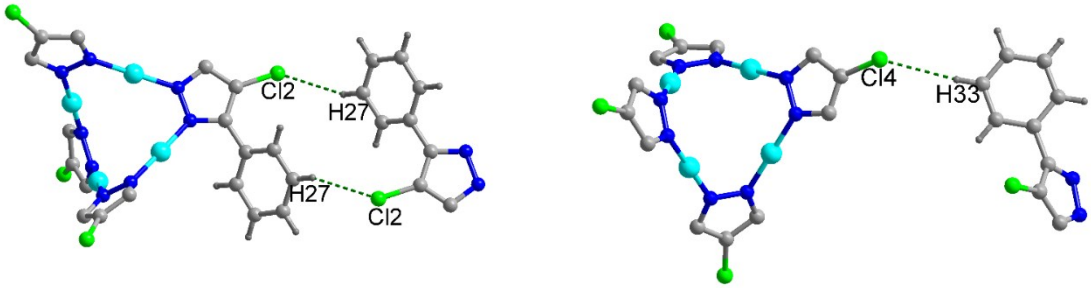

Fig. S13 The intermolecular Cl···H(Ph) interactions in **$(Cu^Ipz)_4$**, some phenyl groups have been omitted for clarity.

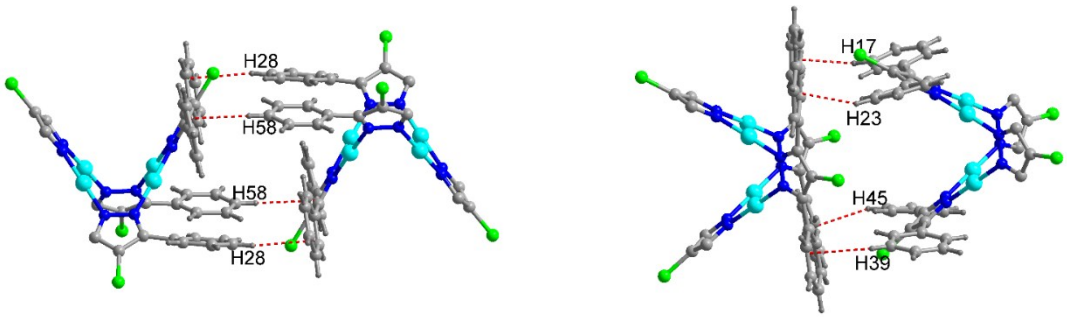

Fig. S14 The intermolecular C-H···π(Ph) interaction in **$(Cu^Ipz)_4$**, some phenyl groups have been omitted for clarity.

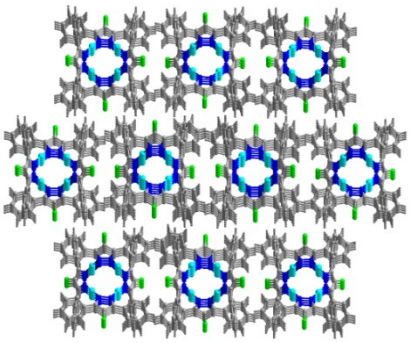

Fig. S15 3-D structure of **($Cu^{I}pz)_4$** formed *via* the intermolecular C-H···π interactions and Cl···H interactions, the solvent molecules have been omitted for clarity.

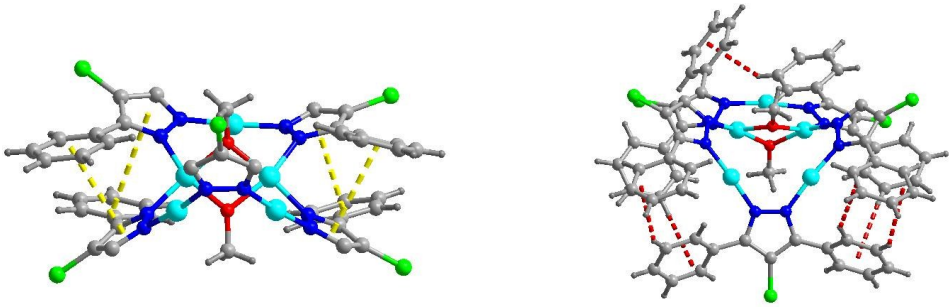

Fig. S16 The intramolecular π(Ph)···π(pz) interaction and C-H···π(Ph) interaction in **$Cu^{I}_3Cu^{II}_2(OMe)_2pz_5$**, some phenyl groups have been omitted for clarity.

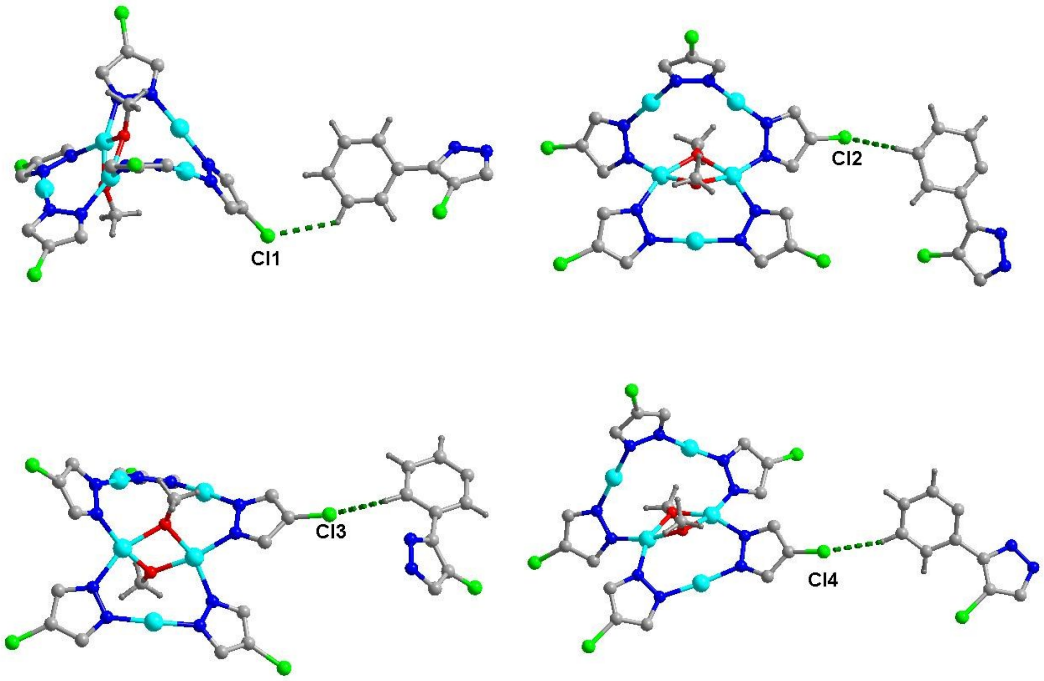

Fig. S17 The intermolecular Cl···H(Ph) interactions in **$Cu^{I}_3Cu^{II}_2(OMe)_2pz_5$**, some phenyl groups have been omitted for clarity.

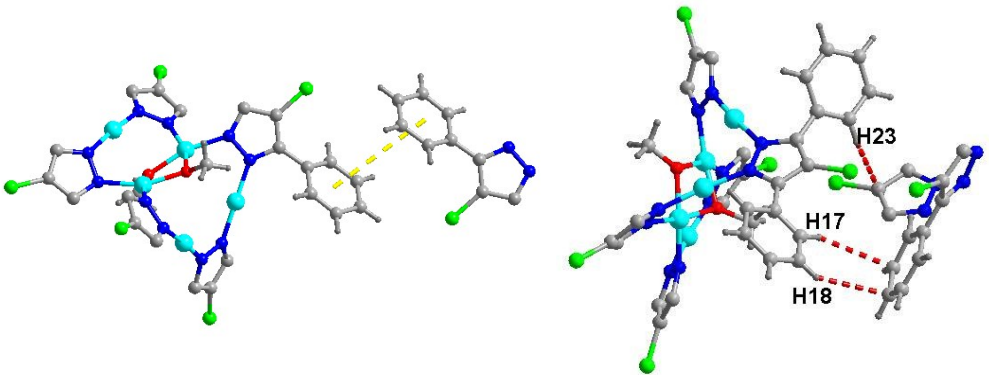

Fig. S18 The intermolecular π(Ph)···π(Ph), C-H···π(Ph) and C-H···π(Pz) interaction in $\mathbf{Cu^{I}_{3}Cu^{II}_{2}(OMe)_{2}pz_{5}}$, some phenyl groups have been omitted for clarity.

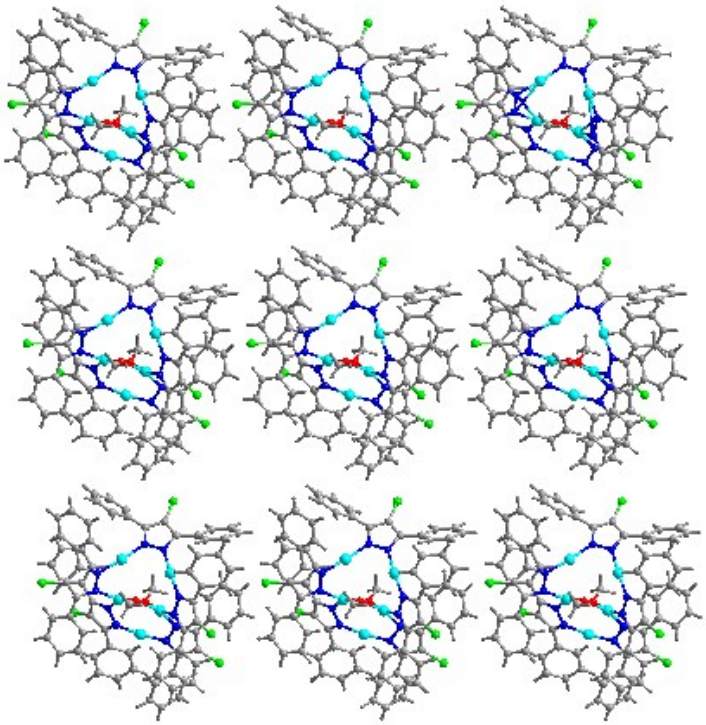

Fig S19 3-D structure of $\mathbf{Cu^{I}_{3}Cu^{II}_{2}(OMe)_{2}pz_{5}}$ formed *via* the intermolecular C-H···π, π(Ph)···π(Ph) and Cl(pz)···H hydrogen bond.

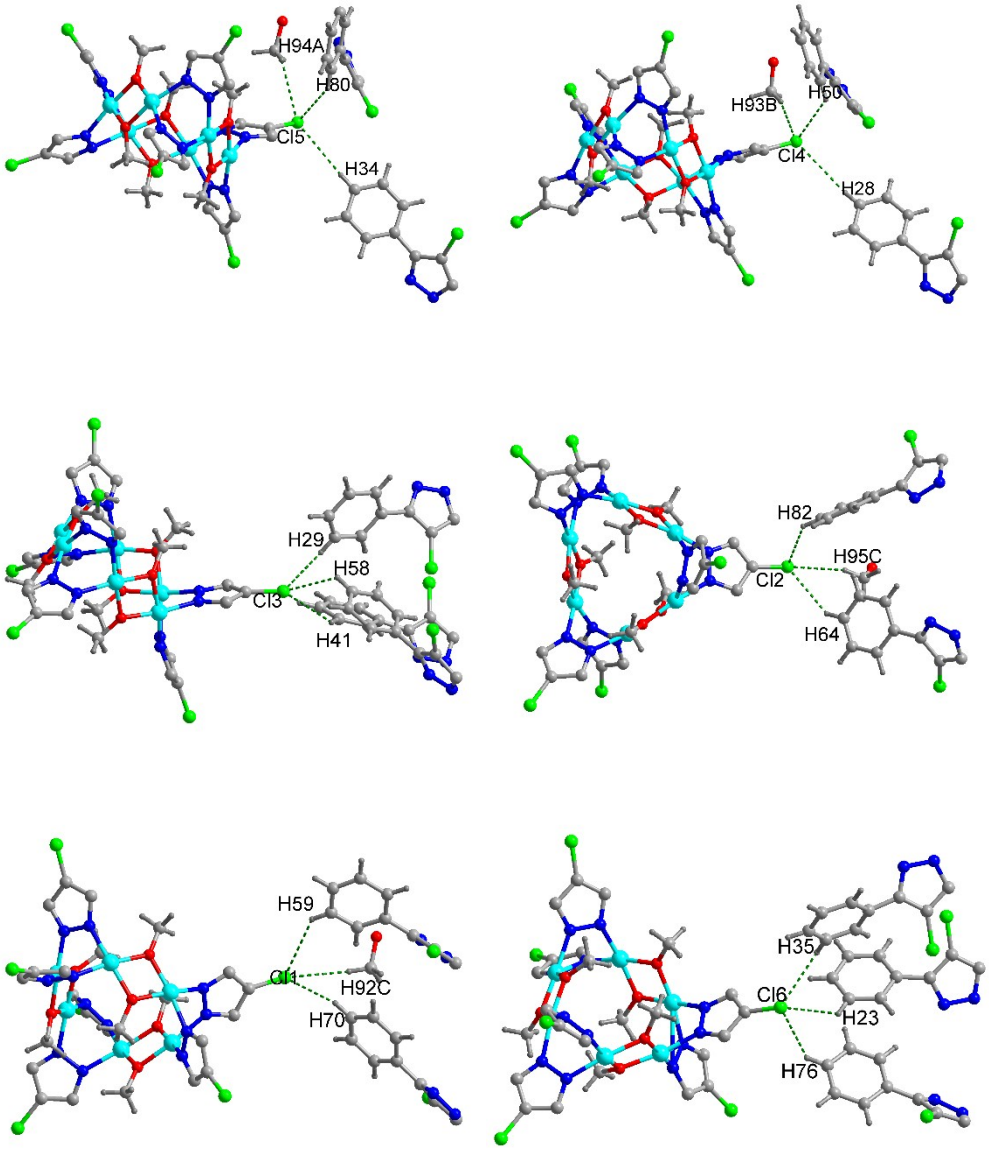

Fig. S20 The intermolecular Cl···H(Ph) interactions in **[Cu^{II}pz(OMe)]$_6$**, some phenyl groups have been omitted for clarity.

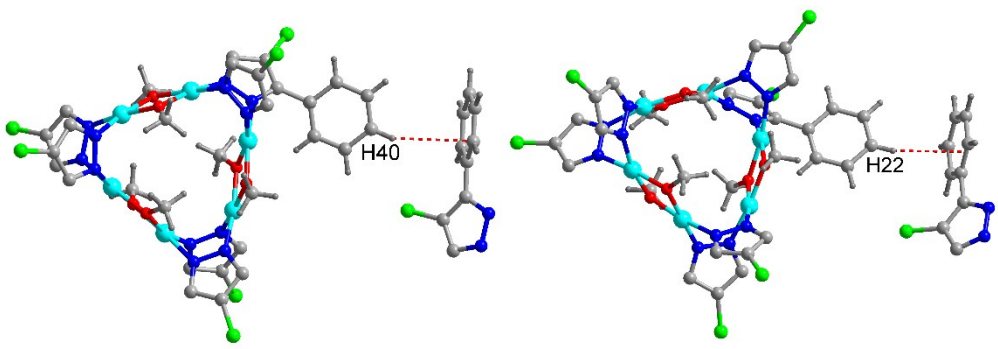

Fig. S21 The intermolecular C-H···π(Ph) interaction in **[Cu^{II}pz(OMe)]$_6$**, some phenyl groups have been omitted for clarity.

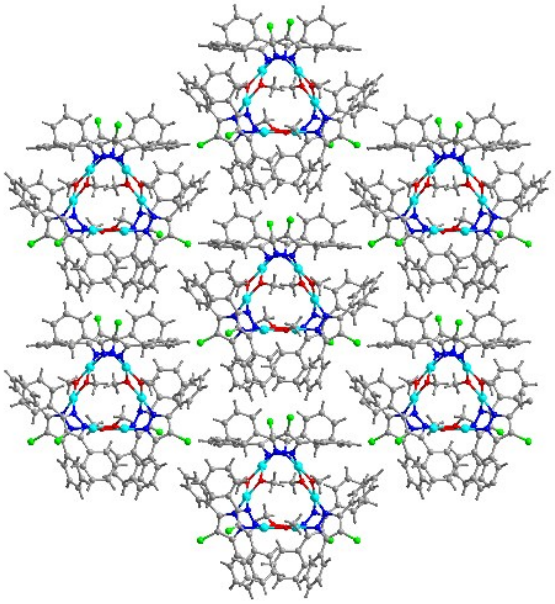

Fig. S22 3-D structure of **[Cu^{II}pz(OMe)]$_6$** formed *via* the intermolecular C-H···π interactions and Cl···H interactions.

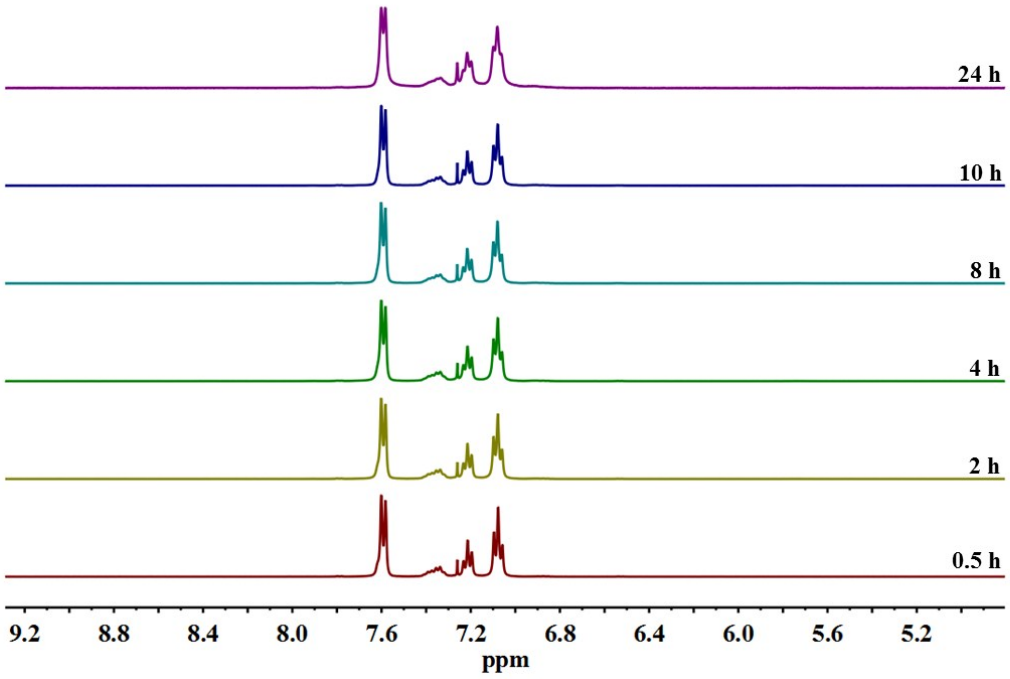

Fig. S23 Stack plot of ^{1}H NMR spectra for **(Cu^{I}pz)$_3$** in $CDCl_3$ at R.T. The sample of **(Cu^{I}pz)$_3$** for NMR spectroscopic measurements was prepared in the glovebox by use of *J. Young* valve NMR tube.

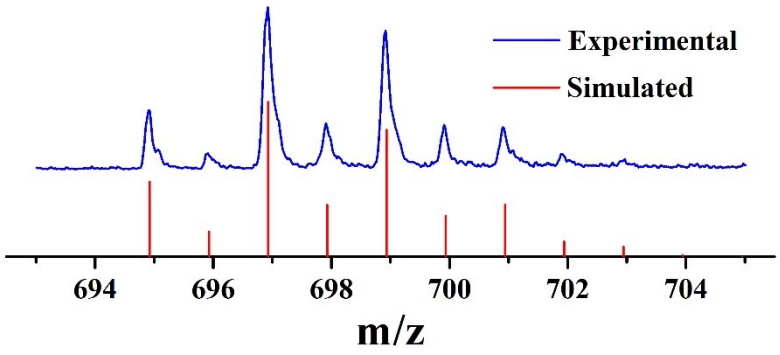

Fig. S24 MALDI-TOF mass spectrum of $[Cu_3pz_2]^+$ with enlargement of the molecular ion peak (696.93 m/z) and its simulated isotopic pattern.

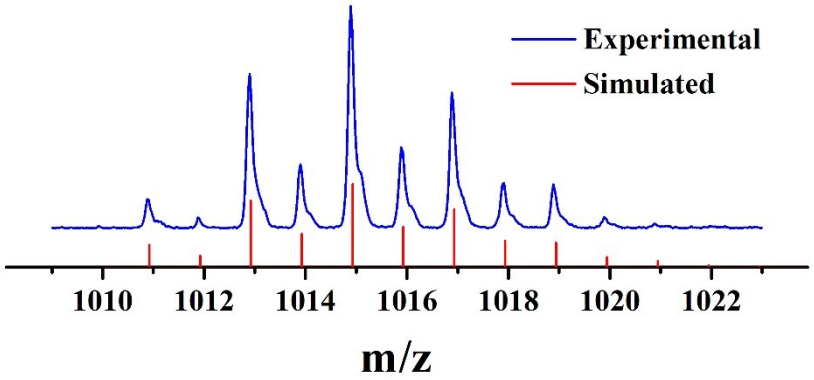

Fig. S25 MALDI-TOF mass spectrum of $[Cu_4pz_3]^+$ with enlargement of the molecular ion peak (1014.90 m/z) and its simulated isotopic pattern.

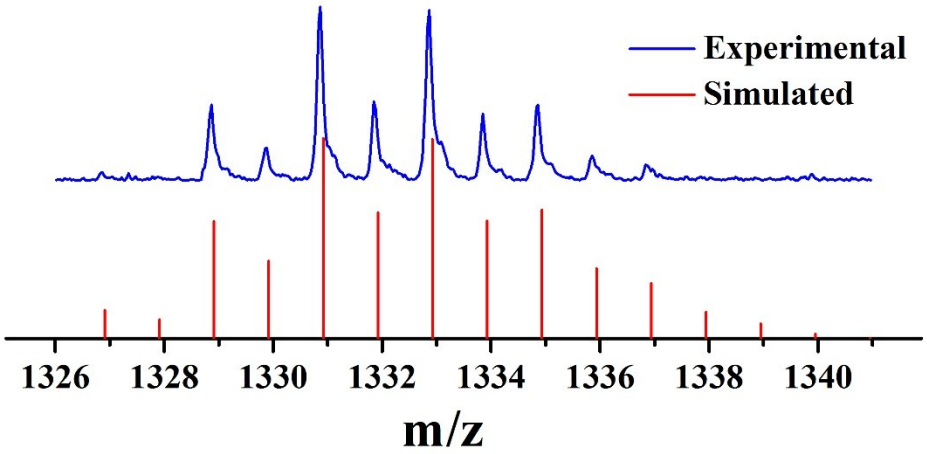

Fig. S26 MALDI-TOF mass spectrum of $[Cu_5pz_4]^+$ with enlargement of the molecular ion peak (1330.96 m/z) and its simulated isotopic pattern.

Table S4 The elemental analysis of **[Cu^{II}pz(OMe)]$_6$** drying in the air for three days.

	C	H	N
[Cu^{II}pz(OMe)]$_6$	55.18	8.04	3.76
experimental	53.93	8.36	3.32
[Cu^{II}pz(OH)]$_6$	53.90	8.38	3.37

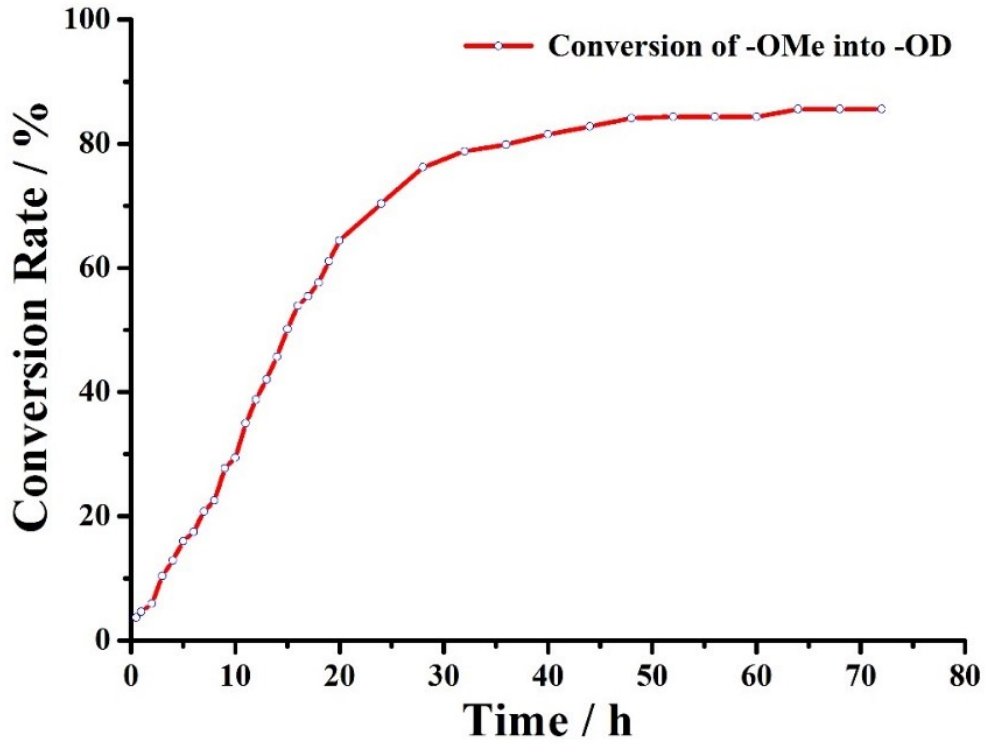

Fig. S27 Conversion curve of OMe^-/OD^- for **[Cu^{II}pz(OMe)]$_6$** soaked in D_2O. Maleic acid was used as standard substance to evaluate the concentration of MeOD released to the solution due to the replacement of OMe^- by OD^-.

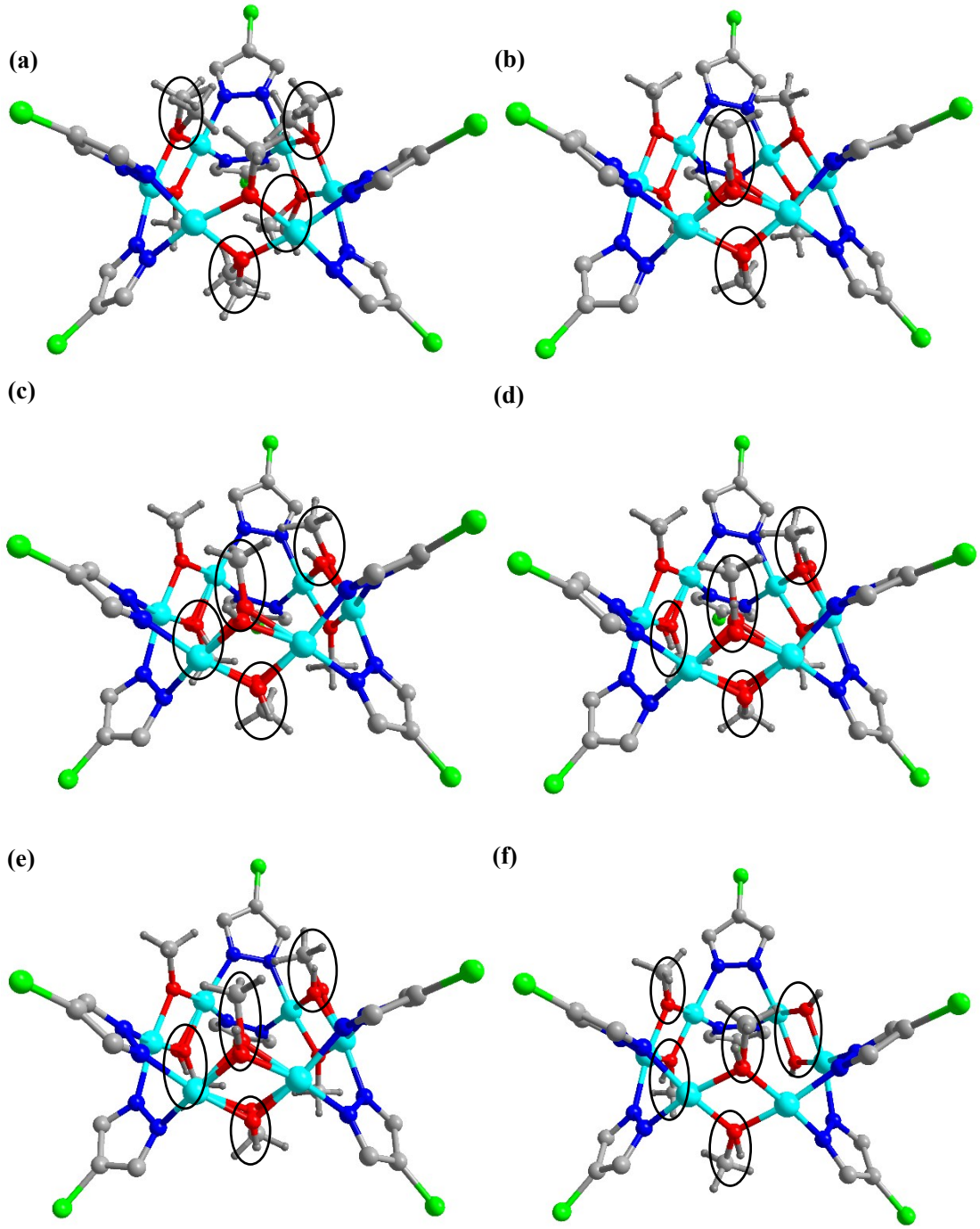

Fig. S28 The ball-and-stick diagram of **[Cu^{II}pz(OMe)]$_6$** which was immersed in H_2O for: (a) 12 h; (b) 24 h; (c) 36 h; (d) 48 h; (e) 72 h; (f) 96 h.

Solid State Luminescence Properties.

Considering the attractive photophysical properties exhibited by the similar trimer - [Cu(μ-pz)]$_3$ (pz = substituted pyrazolate anion), so the solid-state luminescence properties of **(Cu^{I}pz)$_3$** have been studied. As shown in Fig. S29, the crystalline sample of **(Cu^{I}pz)$_3$** shows a dual-emission centered at 482 and 531 nm with λ_{exc} ~ 390 nm at RT. In order to understand the origin of emission, the

luminescent spectra of the ligand were recorded under the same conditions. The ligand also shows a dual emissions centered at 485 and 529 nm with λ_{exc} ~ 390 nm (Fig. S30). It is indicated that the emission from **$(Cu^{I}pz)_3$** is mainly ligand-centered.

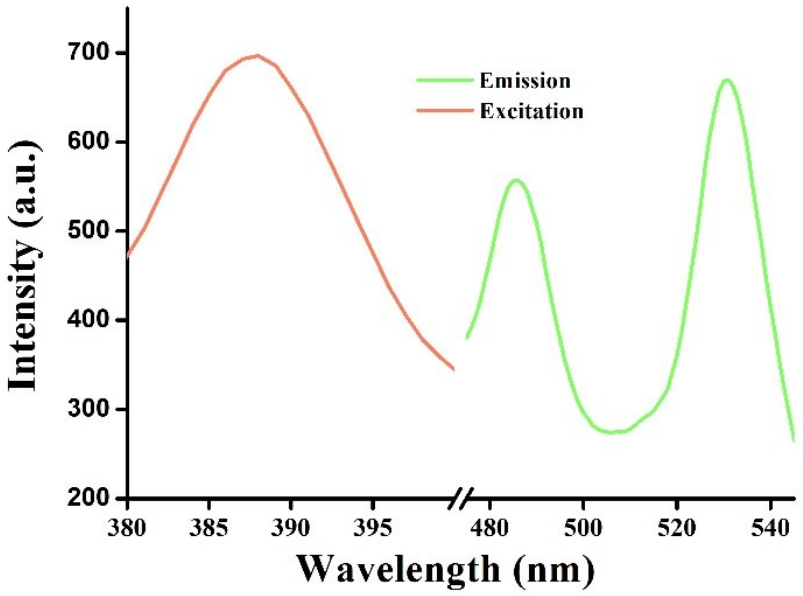

Fig. S29 Emission and excitation spectra of a crystalline sample of **$(Cu^{I}pz)_3$** at RT.

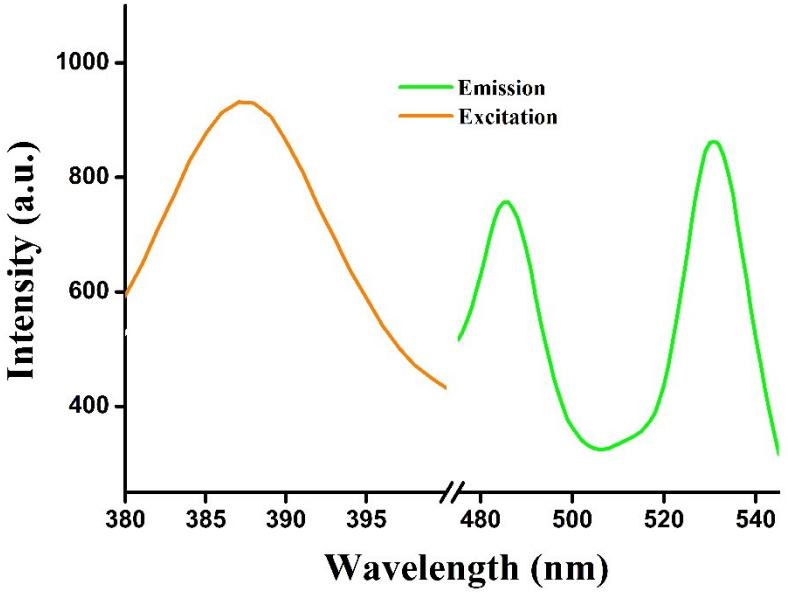

Fig. S30 Emission and excitation spectra of a crystalline sample of 4-chloro 3,5-diphenylpyrazole at RT.